Materials Today Bio 20 (2023) 100679

Contents lists available at ScienceDirect

Materials Today Bio

journal homepage: www.journals.elsevier.com/materials-today-bio

Intracellular hydrogelation of macrophage conjugated probiotics for hitchhiking delivery and combined treatment of colitis

Jingzhe Wang [a,1], Dini Hu [b,1], Qian Chen [c,1], Tonggong Liu [a], Xiaoting Zhou [d], Yong Xu [a], Hongzhong Zhou [a,**], Dayong Gu [a,***], Cheng Gao [a,*]

[a] Department of Laboratory Medicine, Shenzhen Institute of Translational Medicine, The First Affiliated Hospital of Shenzhen University, Shenzhen Second People's Hospital, Shenzhen, 518035, China
[b] CAS Key Laboratory of Animal Ecology and Conservation Biology, Institute of Zoology, Chinese Academy of Sciences, Beijing, 100101, China
[c] Center for Evolution and Conservation Biology, Southern Marine Science and Engineering Guangdong Laboratory (Guangzhou), Guangzhou, 511458, China
[d] Yulin Center for Food and Drug Control, Yulin, 719000, China

ARTICLE INFO

Keywords:
Cell-based delivery
Anti-inflammation
Intestine retention
Probiotics
Colitis

ABSTRACT

Immune cell membrane coated nanomedicine was developed to neutralize cytokines via receptor-ligand interaction, which showed potential for the treatment of inflammatory bowel disease (IBD). However, cell membrane isolation and re-assembly process involved protein loss and spatial disorder, which reduced the sequestration efficiency towards cytokines. In addition, oral administration of probiotics was accepted for IBD treatment via gut microbiota modulation, but most probiotics showed weak adhesion to intestine mucosa and were quickly expelled from gastrointestinal tract. Herein, an intracellular hydrogelation technology was proposed to construct gelated peritoneal macrophage (GPM) with intact membrane structure, resulting from the avoidance of membrane isolation and re-assembly process. GPM efficiently neutralized multiple cytokines *in vitro* and *in vivo* to ameliorate inflammatory Caco-2 cells and colitis rats by regulating oxidative stress, inflammation level and intestinal barrier repair. Moreover, the probiotics (Nissle1917, EcN) were easily attached on GPM surface through specific recognition, to construct GPM-EcN conjugate for GPM hitchhiking delivery to colitis tissue. Conjugation process of GPM and EcN showed no damage on bacterial physiological function. Due to the chemical attachment on inflammatory cells, GPM carried the attached EcN hand-in-hand to accumulate in the colitis tissue of IBD rat, and enhanced intestine retention time of EcN in comparison to free EcN, which improved bacterial diversity, and shifted the microbiota community and acid metabolites to an anti-inflammatory phenotype. This study transferred the hydrogel synthesis from *in vitro* to intracellular cytoplasm, and came to a new insight of conjugating strategy of GPM and probiotics for hitchhiking delivery and combined anti-IBD treatment.

1. Introduction

Inflammatory bowel disease (IBD) was a chronic inflammatory condition of the gastrointestinal tract, and emerging as a global public health problem. [1,2] It was always associated with continuous diffusive gut epithelial inflammation and altered gut microbial composition, including ulcerative colitis and Crohn's disease. [3,4] Although the precise etiology of IBD remained unknown, intestinal epithelial cells were understood to be regulated by immune cells beneath the intestinal epithelial monolayer via cytokines, such as tumor necrosis factor-α (TNF-α) and interleukin (IL)-1β. [5,6] Especially, TNF-α and IFN-γ could directly affect the epithelial permeability and the capacity for electrogenic ion transport of intestinal epithelial cells. [7] Thus, much progress had been achieved in the anti-inflammation therapy to relieve IBD symptom, and monoclonal antibodies, such as anti-TNF-α antibody and anti-IL-1β antibody, were widely used for patients who failed conventional medical therapy. [8,9] It was highly effective for induction and maintenance of clinical IBD remission. [10,11] However, inflammatory bowel involved various

* Corresponding author.
** Corresponding author.
*** Corresponding author.
E-mail addresses: zhouhongzhong@email.szu.edu.cn (H. Zhou), wanhood@email.szu.edu.cn (D. Gu), chenggao@email.szu.edu.cn (C. Gao).
[1] These three authors contributed equally to this work.

https://doi.org/10.1016/j.mtbio.2023.100679
Received 8 March 2023; Received in revised form 15 May 2023; Accepted 19 May 2023
Available online 19 May 2023

inflammatory cytokines, and one antibody or their mixture only accelerated the clearance of corresponding inflammatory factor or a few of them. The other cytokines related to disease characteristics also existed and continuously caused damage on intestinal epithelial cells. To obtained a better anti-inflammation therapy on IBD, multiple neutralization strategy towards diverse disease-related cytokines was desirable for patient who required biological treatment.

Immune cell could be activated by different inflammatory cytokines through receptor-ligand mediated signal pathway [12,13] Thus, a large number of studies reported that immune cell membrane coated nanomedicine could sequestrate and neutralize multiple cytokines via receptor-ligand interaction. [14,15] Cell biomimetic nanomedicine is emerging as a novel biomimetic drug delivery system, and many researchers develop various cell membrane coated nanomedicine, which camouflaged the synthetic nanoparticle to avoid clearance by monocyte phagocytic system. [16,17] In addition, those membrane coated nanoparticles inherit the biological functions unique of cell membranes, and also have membrane receptors such as Toll-like receptor family and interferon receptor, tumor necrosis factor receptor, to neutralize inflammatory factors via receptor-ligand interaction. [18,19] However, cell membrane must be collected from source cell firstly, and then re-assembly on the template nanoparticle via extrusion method. The preparation process was always accompanied by membrane protein loss and protein spatial disorder, which led to a low cytokine neutralization efficiency. Nevertheless, the interaction between these cytokines with immune cell membrane proved a design cue for an action mechanism-targeted anti-inflammation platform. Thus, dead immune cell with intact membrane structure would have the potential to functionalize as a universal “cellular sponge” to efficiently capture and neutralize different types of cytokines. This might provide a new insight for efficient anti-inflammation treatment toward multiple cytokines, which avoid the membrane isolation and re-assembly process in the preparation of cell membrane coated nanomedicine.

In addition to intestinal inflammation, the gut microbiota alteration in IBD pathogenesis had been recently highlighted in many researches. [20,21] It was accepted that gut microbiota helped metabolize substances and contributed to human health via supporting various metabolites. [22] Dysbiosis of gut microbiota was found in IBD patients and mice colitis models. [23] Thus, the approaches of gut microbiota-based therapy had been developed for prevention and treatment of IBD, and many good evidences were presented to show their effect on the amelioration of colitis in animal models (mouse and rat) and even IBD patients. [24–26] This indicated that gut microbiota would be a promising therapeutic target for IBD treatment, such as the probiotic therapy in clinical practice. However, conventional oral administration of probiotics exhibited very low utilization rate due to the limited intestine accumulation. [27,28] Most bacteria had a weak adhesion ability to intestine endothelial cells, and were quickly expelled from the intestinal tract. [29] It was essential to enhance the adhesion interaction between oral probiotics with intestinal mucosa, and thereby increased the accumulation time in intestinal tract for an effective regulation on gut microbiota. Regarding the chemical attachment on inflammatory cells, dead immune cell specifically bound to colitis mucosa for long time retention in colon. Due to the specific recognition between immune cells and bacteria, dead immune cell with intact membrane structure might also absorb bacteria through the interaction between Toll-like receptor (TLR) of immune cell membrane and lipopolysaccharide (LPS) of bacterial cell. This conjugation strategy of dead immune cells and probiotics potentially prolonged the residence time in colon tissue, and addressed the issue of quick bacteria clearance.

In order to maximize the neutralization efficiency of dead immune cells toward multiple cytokines in IBD, this study proposed an intracellular gelation strategy to construct gelated peritoneal macrophage (GPM), which exhibited the macrophage-like morphology and maintained intact membrane structure without membrane protein loss and spatial disorder. There are many receptors on the surface of macrophages such as scavenger receptors, toll-like receptors (TLRs) and cytokine/chemokine receptors, and external stimulus factors (such as CD163, TNFα and IL-1) could bind with macrophage through receptor-ligand interaction to activate the downstream signal pathway. [30,31] In vitro cytokine sequestration revealed an efficient neutralization effect of GPM toward various cytokines via receptor-ligand interaction. Furthermore, Nissle1917 (EcN) was chosen for microbiota-based therapy, and conjugated on GPM surface via specific binding between TLR and LPS on the membrane of GPM and EcN (Fig. 1), without any damage on the bacterial physiological function. Due to the chemical attachment on colitis mucosa, GPM went hand-in-hand with the attached EcN to accumulated in colitis tissue of IBD rat, and prolonged the intestine retention time of EcN. After oral administration of GPM-EcN, inflammation and intestine damage of IBD rat were significantly ameliorated, and intestinal flora and metabolite analysis showed the dysbiosis of gut microbiota was recovered to normal condition. This study provided a novel conjugating strategy of GPM and probiotics for hitchhiking delivery to inflammatory intestine, and exhibited combinational anti-IBD therapy via cytokine neutralization of GPM and gut microbiota recovering of EcN.

2. Methods and materials

2.1. Materials

PEG-DA (molecular wight 700 Da), I2959, and LB broth medium were purchased from Aladdin (China). LPS and TNBS were purchased from Sigma-Aldrich (USA). DiI were purchased from Beyotime Biotechnology (China). *Escherichia coli* Nissle 1917 (Cat No. ST12134) was obtained from Kerui Sibo (China).

Raw264.7 cell was supplied by ATCC (USA), and identified by DNA fingerprinting, isozyme detection and mycoplasma detection. Fetal Gibco Dulbecco's modified Eagle's medium (DMEM), Roswell Park Memorial Institute (RPMI) 1640 medium, trypsin-EDTA (0.25%) and foetal bovine serum (FBS) were purchased from Gibco (USA). Claudin 1 antibody (Proteintech, Cat No.: 13050-1-AP), E-cadherin antibody (Proteintech, Cat No.: 20874-1-AP), MPO antibody (Proteintech, Cat No.: 22225-1-AP), SNAI1 antibody (Proteintech, Cat No.: 13099-1-AP), vimentin antibody (Proteintech, Cat No.: 10366-1-AP), F4/80 antibody (Proteintech, Cat No.: 29414-1-AP), CD86 antibody (Proteintech, Cat No.: 13395-1-AP) and CD206 antibody (Proteintech, Cat No.: 18704-1-AP) were get from Proteintech (China). Elisa kits for detection of TNF-α, IL-1β and MPO were obtained from Servicebio (China).

SD rat was collected from Shenzhen Charles River. All animal experiments were approved by the Animal Ethics Committee, Shenzhen Second People's hospital and were conducted in accordance with the Animal Management Rules of the Ministry of Health of the P. R. China.

2.2. Isolation of peritoneal macrophages

Rat peritoneal macrophages were collected from the peritoneal cavity of SD rat. 10 mL of DMEM was injected into rat peritoneal cavity, and rat abdomen was gently rubbed for 2 min. Then, the abdominal fluid was collected after further placement for 7 min, and centrifugated to obtain monocytes. The precipitated monocytes were dispersed in 10 mL of DMEM containing 10% FBS, penicillin (100 U/mL), and streptomycin (100 μg/mL), and incubated for 12 h. Finally, the floating cells were removed and the adherent cells were the peritoneal macrophages, and the membrane markers (F4/80 and CD11b) were checked by flow cytometry.

2.3. Intracellular gelation of peritoneal macrophages

Peritoneal macrophages were dispersed in PBS solution containing 10% (wt%, weight percent) of PEG-DA and 0.1% (wt%) of I2959. After placement in −80 °C fridge for 10 min, the cell solution was quickly frozen and take out for natural melting. Then, macrophage was collected

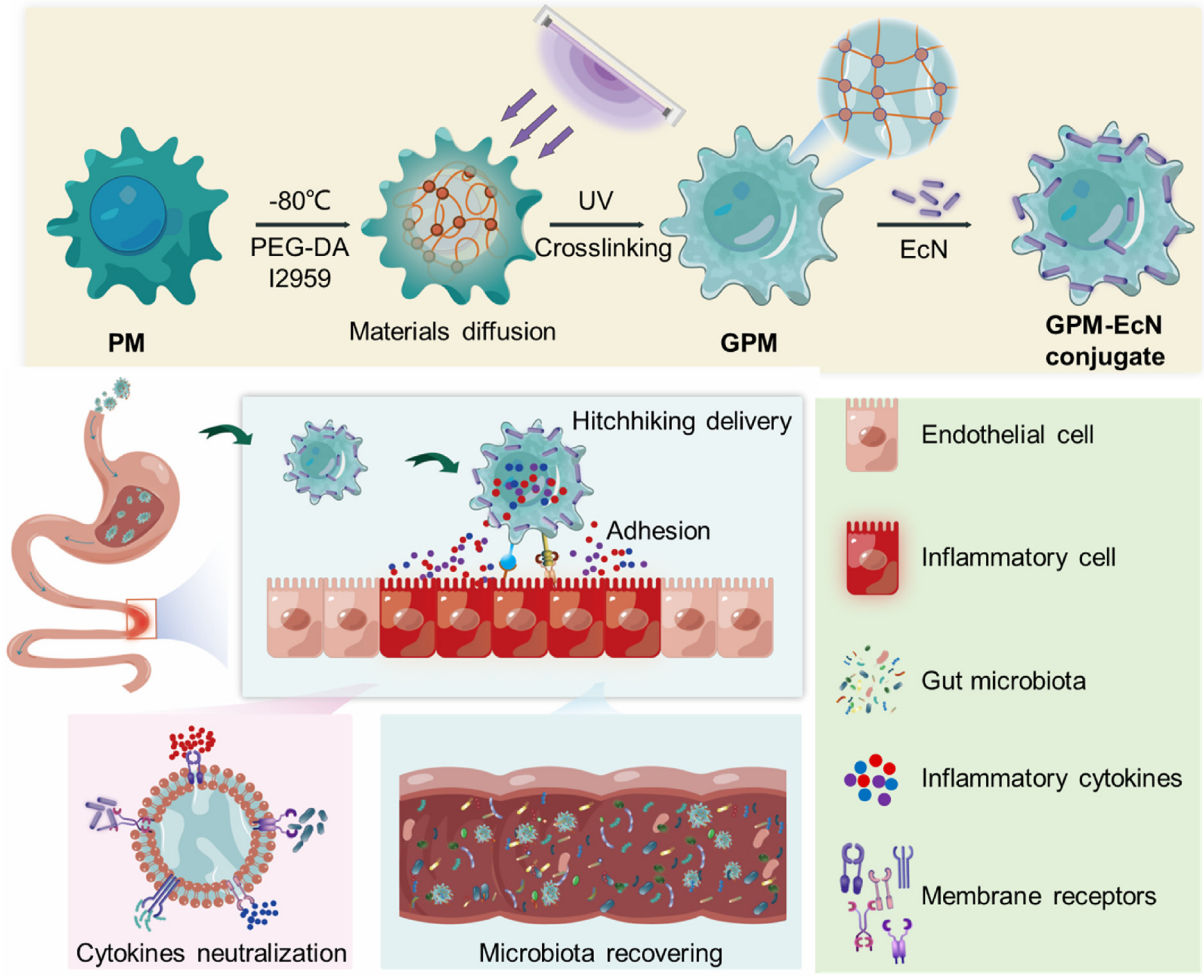

Fig. 1. Schematical illustration of GPM-EcN for targeted treatment of IBD rat via cytokine neutralization and microbiota recovery. GPM was prepared via intracellular hydrogelation to maintain the intact membrane structure without membrane protein loss and spatial disorder, and bound with EcN to construct GPM-EcN through the special recognition of TLR in GPM membrane and LPS in EcN membrane. Due to the inflammatory tropism, GPM went with the attached EcN hand-in-hand to accumulated in the colitis tissue via oral administration, and prolonged the colon retention time of EcN. Then, GPM efficiently sequestrated and neutralized proinflammatory cytokines via receptor-ligand interaction, and EcN recovered the gut microbiota normalization. Finally, GPM-EcN conjugate restored intestinal homeostasis in the colitis rat by regulating oxidative stress, inflammation level, intestinal barrier repair, gut microbiota and acid metabolites.

and washed with PBS quickly to remove extracellular PEG-DA and I2959. Under UV irradiation (15W) for 15 min, the intracellular hydrogel was formed and gelated peritoneal macrophage was obtained.

2.4. Effect of GPM on LPS-infected Caco-2 cells

Caco-2 cells obtained from the ATCC (USA) and cultured in DMEM (Gibco) containing 10% FBS (Gibco), 1% non-essential amino acids and 1% glutamine. Caco-2 cells were co-treated with 1 mg/mL of LPS and different concentrations of GPM (10, 20, 40, 80, 160, 320, 640, and 1280 μg/mL) for 24 h, and the cell viability was measured by MTT assay. Then, Caco-2 cells were co-treated with 1 mg/mL of LPS and 320 μg/mL of GPM for 24 h, and the concentrations of inflammatory cytokines (TNF-α and IL-1β) in media were determined by Elisa kits. An epithelial volt-ohmmeter was used for the detection of transepithelial electrical resistance (TEER) of filter-grown Caco-2 intestinal monolayers as previously reported, [32] and TEER of Caco-2-plated filters was measured daily. After treatment with 1 mg/mL of LPS and 320 μg/mL of GPM for 12 h, Caco-2 cells were stained by DCFH-DA for ROS detection, and imaged by confocal laser scanning microscope (CLSM) and quantified by flow cytometry.

2.5. WB analysis on membrane protein of GPMs

Membrane protein was isolated form GPMs and PMs by membrane isolation kit, and quantified by BCA assay. Equal amounts of membrane protein were subjected to WB analysis. Briefly, protein sample was separated by 10% sodium dodecyl sulfate polyacrylamide gel electrophoresis (SDS-PAGE) and transferred to polyvinylidene difluoride membranes. Then, polyvinylidene difluoride membrane was blotted for specific antibodies, including TNFR2 antibody (Proteintech, Cat No. 19272-1-AP), IL1R2 antibody (Proteintech, Cat No. 60262-1-Ig), TLR4 antibody (Proteintech, Cat No. 19811-1-AP) and TLR2 antibody (Proteintech, Cat No. 17236-1-AP), using an enhanced chemiluminescence method (GE Healthcare). Finally, the immunoblots of specific bands were obtained by using a Multi Spectral imaging system, and quantified by densitometric analysis.

2.6. Conjugation of GPM and E. coli

320 μg/mL of GPMs was incubated with 10^7 CFU/mL of EcN for 2 h on the shaker, and the obtained solution was centrifugated at 1000 xg for 5 min. The precipitated mixture was observed in confocal laser scanning

microscope (CLSM) and scanning electronic microscope (SEM). M1 polarization ($F4/80^+CD86^+$ cells) rates of GPM and PM were measured by flow cytometry. The precipitated mixture was incubated in LB culture for different times (0, 2, 4, 6, 8, 12, 16, 24 h), and the optical density of resulting solution was measured by microplate reader at a wavelength of 600 nm. In addition, 10^7 CFU/mL of EcN solution was incubated with different concentrations of GPM (10, 20, 40, 80, 160, 320, 640, and 1280 μg/mL), respectively. After incubation on the shaker for 2 h, the resultant solution was centrifuged to remove GMPs, and the remaining EcN inoculated in agar plate and the number of bacterial colonies was counted.

2.7. Cytokine sequestration and inflammation inhibition effect of GPMs

1 mL of TNF-α (10 nm/mL) and IL-1β (10 nm/mL) was added with different concentrations of GPM (10, 20, 40, 80, 160, 320, 640, and 1280 μg/mL). After incubation for 3 h, the resulting solution was centrifuged to remove GMPs, and the supernatant concentrations of TNF-α and IL-1β were detected by Elisa kits. In addition, macrophage was co-treated with 1 mg/mL of LPS and 320 μg/mL of GPMs for 24 h. M1 polarization ($F4/80^+$ $CD86^+$ cells) rate was measured by flow cytometry.

2.8. Construction of IBD rat model

250 g of Male SD rats were fasted with ad libitum access to water for 24 h, and anesthetized with 30 g/L pentobarbital. Then, SD rat was inserted with a silicone catheter into intestine 8 cm from the anus, and 2% TNBS (10 mL of 5% TNBS, 10 mL of ethanol, 5 mL of saline) was injected into the catheter at a dose of 100 mg/kg. After administration for 24 h, IBD rat model was constructed for future experiments.

2.9. Interaction of GPMs with intestine of IBD rat

After injection of TNBS for 3 days, IBD rats were intragastrically administered with free Cy5 and Cy5 loaded GPM (Cy5-GPM) at a dose of 1 mg/kg (n = 3), and the colon tissues were collected for IVIS imaging after administration for different times (6 h, 12 h and 24 h). Then, the other batch of IBD rats was intragastrically administered with EcN and GPM-EcN at 10^8 CFU/kg of EcN. Recombinant EcN expressing green fluorescent protein (GFP) and GPM stained with red membrane fluorescent dye (DiI) were used to track the *in vivo* biodistribution. After administration for 12 h, 24 h and 36 h, the intestine was collected from treated rat and fluorescently imaged by *in vivo* imaging system (IVIS). EcN exhibited green fluorescence with a Ex/Em of 395/475 nm. GPM showed red fluorescence with a Ex/Em of 549/565 nm.

2.10. Therapeutic evaluation of GPMs on IBD rat

Starting 1 day after the initiation of TNBS-induced inflammation, IBD rat were randomly and blindly separated into four groups (n = 3), and intragastrically administered with saline, EcN, GPM and GPM-EcN at 10^8 CFU/kg of EcN and 70 mg/kg of GPM once every two days with a total of three doses. Normal rat served as positive control group. During the treatment, body weight and stool consistency were recorded every two days with a total of 12 days. At endpoint of treatment (Day 12), rat was sacrificed, and colon was collected for imaging and length measurement. The level of, TNF-α, IL-1β, and MPO in colon tissue was detected by Elisa kits according to the manufacturer's instructions. Colon tissue was fixed by 4% paraformaldehyde (PFA) and embedded in paraffin for section. Hematoxylin and eosin (H&E) and Masson trichrome staining were conducted on colon section, and histological image was obtained under light microscopy. The pathologic score of the colonic damage was investigated according to reported morphological criteria. [33]

2.11. Immunohistochemical analysis

Colon tissue was fixed by 4% paraformaldehyde (PFA) and embedded in paraffin for section. Then, colon section was permeabilized by 0.1% of Triton X-100 for 20 min and blocked by 5% BSA for 20 min prior to antibody staining. After wash with PBS for three times, the sections were stained with the following antibody groups for 1.5 h: Claudin 1 (Proteintech, Cat No. 13050-1-AP), E-cadherin (Proteintech, Cat No. 20874-1-AP), MPO (Proteintech, Cat No. 22225-1-AP), vimentin (Proteintech, Cat No. 10366-1-AP), F4/80 (Proteintech, Cat No. 29414-1-AP), respectively. Then, colon section was washed with PBS for three times, and further stained with goat anti-rabbit IgG (HRP) and anti-rabbit IgG Fab2 Alexa Fluor 594 for 1 h. Finally, colon section was washed with PBS and observed by using CLSM.

2.12. DNA extraction, library construction and bioinformatic analysis

The E.Z.N.A.® Stool DNA Kit (Omega Bio-tek, Norcross, GA, U.S.) was used to extract the DNA from fecal samples. The V4–V5 region of the bacteria 16S ribosomal RNA gene were amplified by PCR using primers of 515F (5′-barcode- GTGCCAGCMGCCGCGG)-3′) and 907R (5′-CCGTCAATTCMTTTRAGTTT-3′). The condition of PCR was 95 °C for 2 min, followed by 25 cycles at 95 °C for 30 s, 55 °C for 30 s, and 72 °C or 30 s and a final extension at 72 °C for 5 min. PCR reactions were performed in triplicate 20 μL mixture containing 4 μL of 5 × FastPfu Buffer, 2 μL of 2.5 mM dNTPs, 0.8 μL of each primer (5 μM), 0.4 μL of FastPfu Polymerase, and 10 ng of template DNA. The AxyPrep DNA Gel Extraction Kit (Axygen Biosciences, Union City, CA, U.S.) was used to extract and purify the amplicons. After quantified using QuantiFluor™ -ST (Promega, U.S.), purified amplicons were pooled in equimolar and paired-end sequenced (2 × 250) on an Illumina MiSeq platform according to the standard protocols. Raw fastq files were demultiplexed, quality-filtered using QIIME (version 1.9.1). The un-assembled reads were discarded. Operational Units (OTUs) were clustered with 97% similarity cutoff using UPARSE (version 11) and chimeric sequences were identified and removed using UCHIME. The taxonomy of each 16S rRNA gene sequence was analyzed by RDP Classifier (version 2.13) against the silva 138 16S rRNA database using confidence threshold of 70%. The raw reads were deposited into the NCBI Sequence Read Archive (SRA) database (Accession Number: PRJNA918512).

2.13. Metabolites extraction and LC-MS/MS analysis

The metabolites extracted from 50 mg fecal samples using a 400 μL of methanol: water (4:1, v/v) solution. The mixture was treated by high throughput tissue crusher Wonbio-96c (Shanghai wanbo biotechnology co., LTD). The samples were settled at −20°Cfor 30min to precipitate proteins. After centrifugation at 13,000 g at 4°Cfor 15min, the supernatant was transferred to sample vials used for LC-MS/MS analysis. The control sample (QC) was prepared by mixing equal volumes of all samples. A Thermo UHPLC system equipped with an ACQUITY BEH C18 column (100 mm × 2.1 mm i.d., 1.7 μm; Waters, Milford,USA) was used to perform the chromatographic separation of the metabolites. A Thermo UHPLC-Q Exactive Mass Spectrometer equipped with an electrospray ionization (ESI) source operating in either positive or negative ion mode was used to collect the mass spectrometric data. After UPLC-TOF/MS analyses, the raw data were imported into the Progenesis QI 2.3 (Nonlinear Dynamics, Waters, USA) for peak detection and alignment. The Human metabolome database (HMDB) (http://www.hmdb.ca/) and Metlin database (https://metlin.scripps.edu/) were used to identify the MS/MS fragments spectra.

2.14. In vivo biosafety evaluation

After treatment for 12 days, the blood and organs (heart, liver, spleen, lung and kidney) were collected from IBD rats. Serum inflammation level (TNF-α and IL-1β) was evaluated by Elisa kits. Serum level of liver function biomarkers (ALT and AST) and kidney function biomarkers (BUN and UA) was analyzed via blood routine examination. In addition,

H&E staining was conducted in sections of heart, liver, spleen, lung and kidney to evaluate the damage condition.

2.15. Statistical analysis

T-test was used for comparison between two columns of date. One-way analysis of variance (ANOVA) was used where three or more columns of data were compared. Two-way ANOVA were utilized where two or more columns of data were compared. Values of $^{*}P \leq 0.05$, $^{**}P \leq 0.01$ and $^{***}P \leq 0.001$ were considered statistical significance. All experiments were repeated at least three times, and all data was shown as the mean ± standard deviation (SD).

3. Results and discussion

3.1. Preparation and cytokine sequestration of GPM

PEG-DA and Irgacure 2959 (I2959) were widely used for photochemical crosslinking of hydrogels. [34,35] In this study, the synthesis of hydrogel was transferred into intracellular cytoplasm. In order to maximize the intracellular infiltration of hydrogel materials before gelation, small molecular weight (600 Da) and low centration (10%, weight percent (Wt %)) of PEG-DA, and 1 wt% of I2959 were therefore chosen, and Fig. S1a exhibited the successful formation of hydrogel with a good swelling property (Fig. S1b). Subsequently, peritoneal macrophage (PM) was collected from rat abdominal cavity, and the purity of rat PM reached ~94.1% (Fig. S2a). After a freeze-thaw treatment with PEG-DA and I2959, the resulting PM was placed on ice surface and irradiated by UV light (1.5W) for 15 min to construct GPM. The cold condition was to avoid protein degradation and denaturation of GPM. After incubation with PBS solution, GPM still maintained the intact cellular morphology even after treatment for 24 h (Fig. 2a), while Non-gelated PM (PM in PBS solution after a freeze-thaw cycle) quickly degraded into cell fragments in 6 h, indicating that intracellular gelation served as cytoskeleton to support the stability of cell structure. Moreover, scanning electronic microscopy (SEM) (Fig. 2b) showed a similar cellular morphology of GPM to PM, but Non-gelated PM lost cellular dimensional shape. In addition, the similar flow scatter plot was observed in GPM and PM (Fig. S2b), further confirming the macrophage-like size of GPM. Then, membrane staining by DiI exhibited completed red fluorescent membrane layer of GPM (Fig. 2c) and showed intact membrane structure. The content of GPM membrane protein was also similar to that of source PM, determined by BCA protein assay (Fig. S2c). The result exhibited there was no membrane protein loss after intracellular hydrogelation process.

Especially, inflammation related receptors in GPM membrane, such as tumor necrosis factor receptor 2 (TNFR2) and interleukin-1 receptor type 2 (IL1R2), were also expressed equally to that of PM membrane under the same cell numbers (Fig. 2d). Due to receptor-ligand interaction, GPM could sequestrate and neutralize diverse cytokines, and Fig. 2e showed a dose-dependence manner in neutralization of TNF-α and IL-1β, with a IC50 (half maximal inhibitory concentration) value of 45.36 μg/mL and 30.48 μg/mL respectively. Moreover, after treatment with 1 mg/mL of LPS for 24 h, PM was polarized into M1 type ($CD86^{+}$ cells), while cotreatment with GPM inhibited the PM polarization (Fig. S3a), showing the potential for *in vivo* anti-inflammation therapy. The result should be attributed to that GPM competitively bound LPS, and thereby reduced the remaining LPS concentration and inhibited PA polarization. On the other hand, PI staining revealed GPM was dead cell (Fig. S2b), and showed no proliferation ability (Fig. S3b). These results indicated that GPM could not be activated to aggravate inflammation when specifically sequestrating multiple cytokines. Further Coomassie staining analysis showed the membrane protein type and content almost did not change between PM and GPM (Fig. S4a). To investigate whether GPM were stable in gastrointestinal tract's low-pH and enzyme-rich environment, GPM was pre-incubated in the simulated gastric fluid (containing HCl solution with pH 1.2 and 1.5x106 U/g of acid-resistant gastric mimic enzyme) for 2 h. As shown in Fig. S4b, GPM was slightly degraded in low-pH and enzyme-rich environment, but most GPM maintained the cell morphology. In addition, the expression of TNFR2 and IL1R2 in GPM membrane was also reduced (Fig. S4c), indicating a moderate degradation of membrane protein of GPM after incubation in simulated gastric fluid. However, the remaining membrane proteins in GPM could still functioned as neutralization agents to sequester multiple proinflammatory cytokines. Collectively, intracellular gelation process not only maintained macrophage morphology, but also did not affect the expression and physiological function of macrophage membrane proteins, especially for those cytokine receptors, which contributed to be a natural reagent of GPM for cytokine neutralization without inflammation activation.

3.2. Protection effect of GPM on Caco-2 cell

Then, human colon cell line (Caco-2 cell) was utilized for *in vitro* study on the treatment of IBD, and the protection effect of GPM was investigated in a classic inflammatory cell model, LPS treated Caco-2 cell. [36] LPS was reported to induce intestinal barrier dysfunction. [37] Consistent with reported literature, [38] LPS treatment (1 mg/mL) significantly reduced transendothelial electrical resistance (TEER) value of Caco-2 cells after incubation for 24 h (Fig. 2f). In contrast, co-treatment with 320 μg/mL of GPM returned the TEER value to normal level, indicating that GPM efficiently protected the intestinal monolayer barrier function. As intestinal barrier function partially depended on the intestinal epithelial cell status, [39] the cell viability of LPS treated Caco-2 cell was studied. As shown in Fig. S5a, only 60% of Caco-2 cell survived after treated with 1 mg/mL of LPS, while co-treatment with GPM significantly increased the rate of cell viability and showed a dose-dependent manner. Moreover, the Lactate dehydrogenase (LDH) measure was utilized to assess cell viability, and LPS treated Caco-2 cell significantly increased LDH release (Fig. 2g), which was alleviated by co-treatment with GPM. These results suggested that GPM had excellent potential for combating LPS-induced intestinal epithelial cell damage.

To reveal the underlying mechanism by which GPM protected intestinal barrier function from disorder, the biological indicators related to oxidative condition, inflammation, and apoptosis state were further evaluated. In consistent with previous studies, LPS treatment induced over expression of reactive oxygen species (ROS), which contributed to the toxic effect on Caco-2 cell. In contrast, co-treatment with GPM obviously ameliorated the oxidative condition, characterized by low DCF fluorescence intensity (Fig. S5b) and decreased DCF level (Fig. S5c). It was well known that LPS activated nuclear transcription factor (NF)-κB and induced proinflammatory cytokine expression, and Fig. 2h confirmed the increased level of TNF-α and IL-1β in Caco-2 cell after LPS treatment. As expected, GPM efficiently combated LPS-induced inflammatory responses in intestinal epithelial cells, due to the neutralization effect towards both inflammatory cytokine and LPS. Collectively, these results demonstrated that GPM was an effective cell-based natural reagent for protecting intestinal epithelial cell from LPS-induced disfunction and cell death, through its excellent anti-inflammatory capacity. Thus, GPM might be an effective adjuvant for treatment of LPS-associated intestinal diseases.

3.3. Construction of GPM-EcN

Toll-like receptors (TLRs) was a well-studied class of receptors presented on macrophages, which mediated the recognition of pathogen-associated molecular patterns (PAMPs) derived from various microbes. [40] As expected, western blot analysis showed the equal expressions of TLR2 and TLR4 in both GPM membrane and PM membrane (Fig. 3a). Lipoteichoic acid and peptidoglycan in gram positive bacteria served as ligand to be recognized by TLR2 in immune cells, and LPS in gram negative bacteria served as ligand to be recognized by TLR4 in immune cells. Subsequently, intestinal probiotic, EcN, were mixture with GPM to

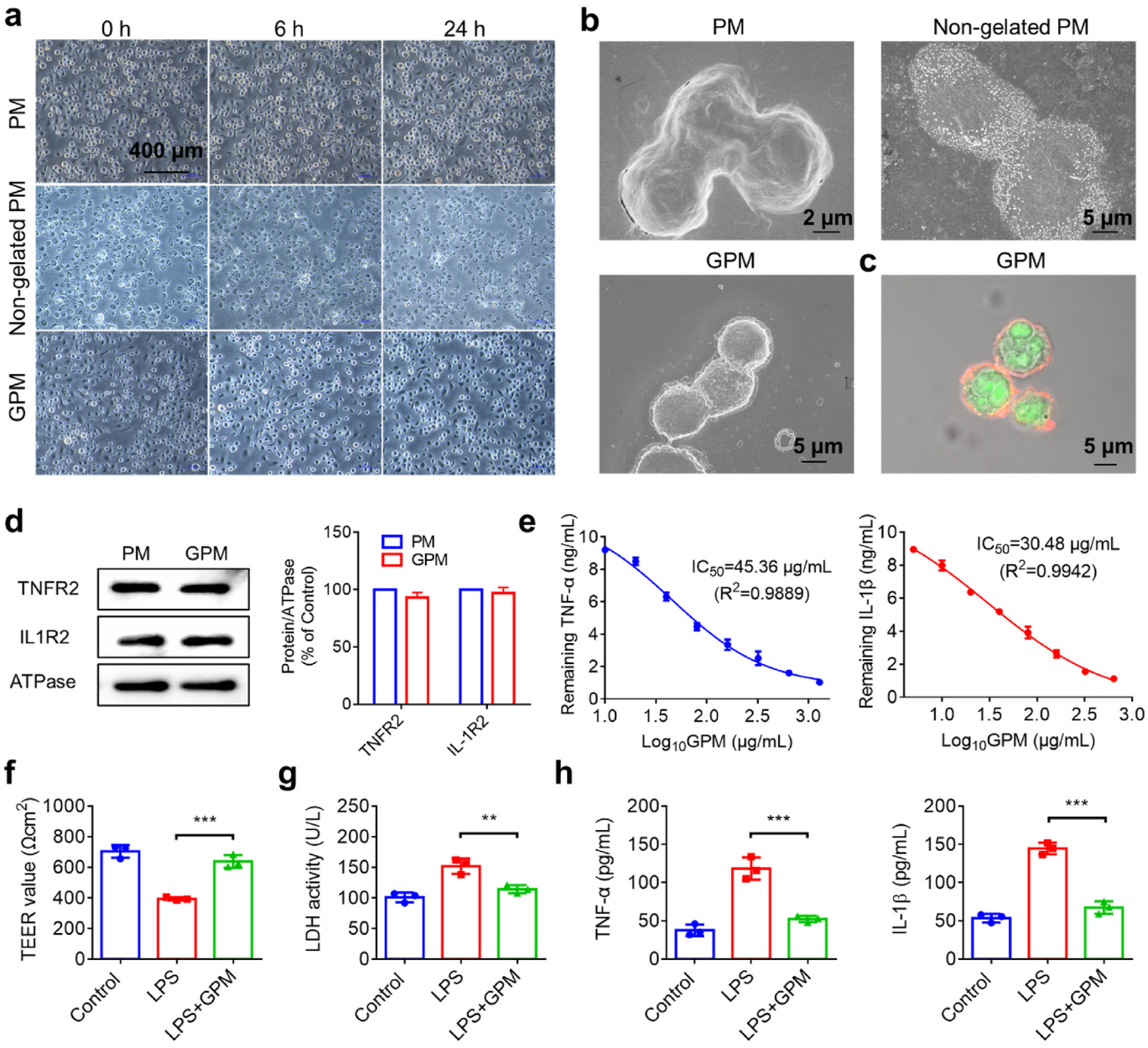

Fig. 2. Characterization of GPM and cytokine sequestration behavior. a) Microscope imaging of PM, Non-gelated PM, and GPM after incubation in PBS for different time points (0, 6 and 24 h). b) SEM imaging of PM, Non-gelated PM, and GPM. c) Membrane labeling of GPM by DiI staining. d) Expression of TNFR2 and IL1R2 in the membrane of PM and GPM, and quantitative result based on the western blot analysis. e) Different concentrations of GPM (10, 20, 40, 80, 160, 320, 640, and 1280 μg/mL) were incubated in PBS solution containing 10 ng/mL of TNF-α and IL-1β, and the remaining cytokine concentrations were determined by Elisa kits. f) Caco-2 cell monolayer was co-treated with 1 mg/mL of LPS (1 mg/mL) and 320 μg/mL of GPM for 24 h, the TEER value was determined by epithelial volt-ohmmeter. g) Caco-2 cell was co-treated with 1 mg/mL of LPS (1 mg/mL) and 320 μg/mL of GPM for 24 h, the LDH release was determined by assay kit. h) Caco-2 cell was co-treated with 1 mg/mL of LPS (1 mg/mL) and 320 μg/mL of GPM for 24 h, the cytokine release of TNF-α and IL-1β were determined by assay kits. Data are represented as the mean ± standard deviation (SD). Two-way ANOVA with multiple comparison test was used for statistical analysis of (d), and One-way ANOVA with multiple comparison test was used for statistical analyses of (f), (g) and (h). **P ≤ 0.01 and ***P ≤ 0.001.

construct GPM-EcN conjugate, and SEM imaging exhibited a number of EcN were conjugated on the GPM surface (Fig. 3b), which should be attributed to the receptor-ligand interaction between TLR4 and LPS. The morphology and structure of conjugated bacteria was maintained in the GPM surface, while EcN incubated with PM only showed bacteria debris in PM surface and most of EcN was degraded. Furthermore, EcN was transformed with green fluorescent protein (GFP) to track the intracellular fate. In Fig. 3c, confocal laser scanning microscopy (CLSM) demonstrated that green fluorescent EcN was located around the GPM, but strong fluorescent intensity was observed inside PM, indicating that most EcN was phagocyted by PM. Then, EcN solution was incubated with different doses of GPM, and the remaining number of bacterial colonies in supernatant was significantly reduced (Fig. 3d). It exhibited a dose-dependent manner with the addition of GPM (Fig. 3e). The proliferation curve revealed the conjugation process in preparing GPM-EcN had no damage on bacterial activity (Fig. 3f). Therefore, due to its lack of cellular activity, GPM easily absorbed EcN to construct GPM-EcN conjugate without any damage on bacterial proliferation. Conversely, the polarization effect of EcN on GPM and PM was also investigated. As shown in Fig. 3g, EcN could promote macrophage polarization into M1

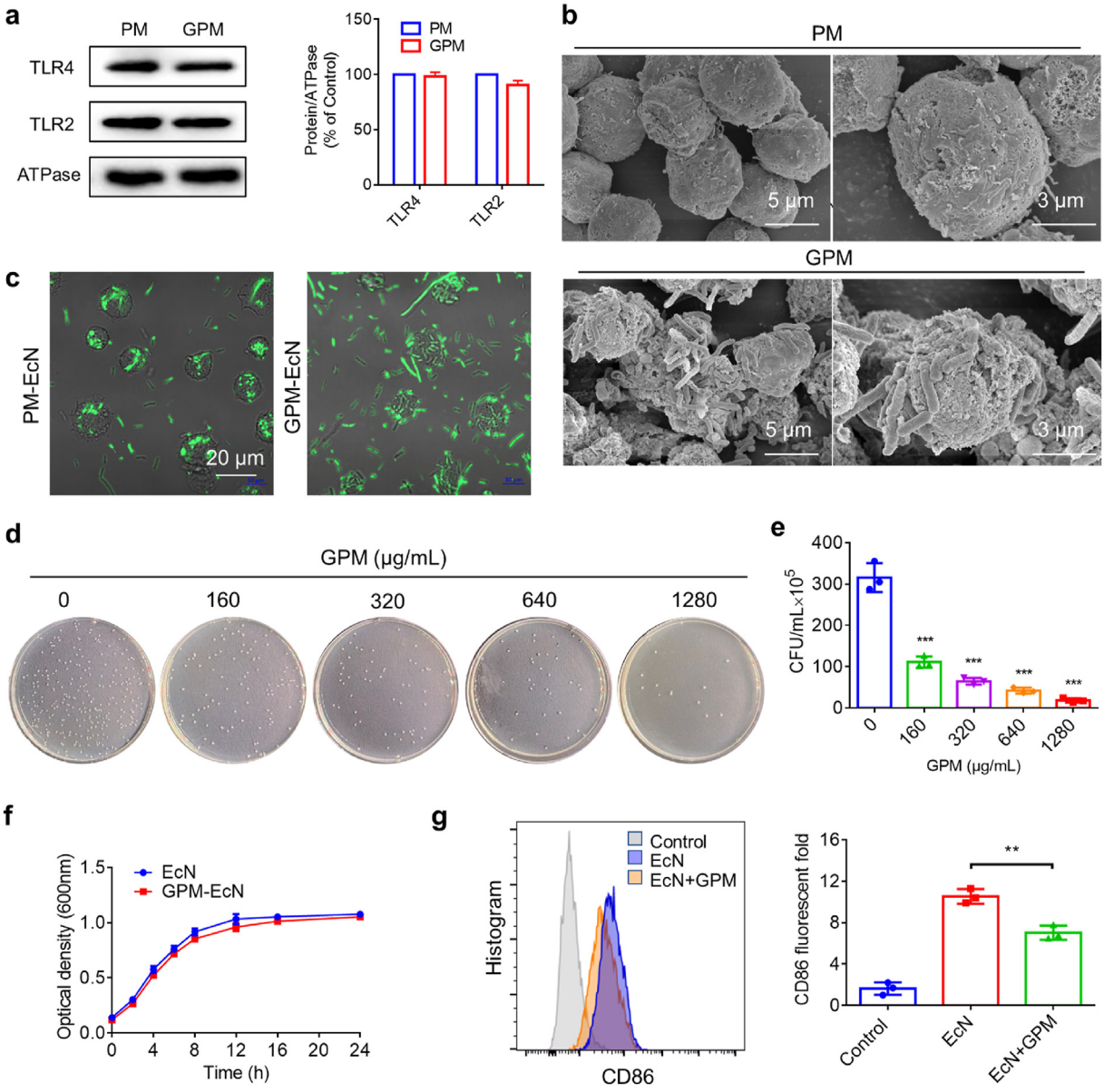

Fig. 3. EcN was absorbed in GPM surface without affecting the physiological function of EcN. a) Expression of TLR4 and TLR2 in the membrane of PM and GPM, and quantitative result based on the western blot analysis. b) CLSM imaging on the mixture of PM and EcN, and GPM-EcN, respectively. Green fluorescence referred to EcN transformed with GFP. c) SEM imaging on the mixture of PM and EcN, and GPM-EcN, respectively. d) 107 CFU/mL of EcN solution was incubated with different concentrations of GPM (10, 20, 40, 80, 160, 320, 640, and 1280 μg/mL) for 2 h, and the remaining number of bacterial colonies in supernatant was observed form agar plate. e) Quantitative of the bacterial colonies. f) Proliferation curve of EcN and GPM-EcN incubated for 24 h. g) Polarization effect of PM and GPM after incubation with EcN, and the percent of M1 macrophage ($F4/80^{+}CD86^{+}$ cell) was quantified by flow cytometry. Data are represented as the mean ± SD (n = 3). Two-way ANOVA with multiple comparison test was used for statistical analysis of (a), and One-way ANOVA was used for statistical analyses of (e) and (g). **P ≤ 0.01 and ***P ≤ 0.001. (For interpretation of the references to color in this figure legend, the reader is referred to the Web version of this article.)

type, but co-treatment with GPM alleviated EcN-induced M1 polarization, which should be attributed to the bacterial sequestration effect of GPM. Collectively, intracellular gelation technology provided a facile methodology that ensured the intact cell membrane structure and contributed to the bacterial sequestration effect of GPM for construction of GPM-EcN conjugate, without affecting the bacterial activity.

3.4. Enhanced intestine retention of EcN

Regarding the specifical recognition and phagocytic effect of macrophage to inflammatory cells, *in vitro* adhesion of GPM to inflammatory Caco-2 cell was firstly studied. LPS treated Caco-2 cell was stained with a green fluorescence membrane dye (DiO), and GPM was stained with a red fluorescence membrane dye (DiI), to track their recognition. As shown in Fig. 4a, a large number of red GPMs were conjugated to green inflammatory Caco-2 cells, and formed heterogenous conjugation. In contrast, red GPM would not couple with normal Caco-2 cell, and only individual cells were randomly located. Moreover, the adhesion efficiency of GPM and inflammatory Caco-2 cell was quantified by flow cytometry. The upper left quadrant and the bottom right quadrant of scatters in control group referred to GPM and normal Caco-2 cell, respectively (Fig. 4b). A data cluster located in the upper right quadrant of scatters plotting, indicating the adhesion of both fluorescence labeled cells. In contrast, when Caco-2 cell was pretreated with LPS, a large data cluster appeared in the upper right quadrant of scatters plotting, and the adhesion efficiency between GPM and inflammatory Caco-2 cell

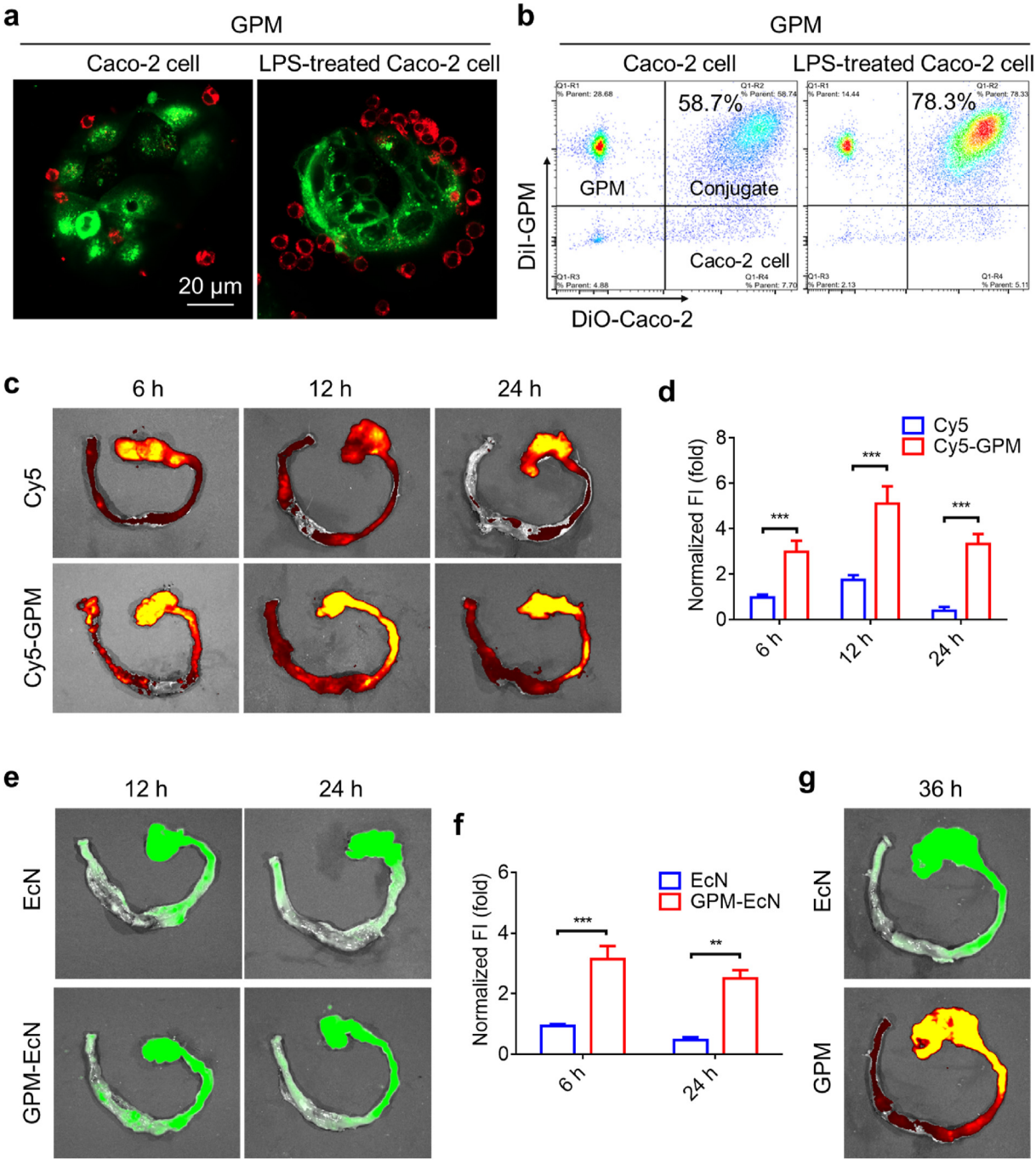

Fig. 4. GPM adhered in the inflammatory colon and prolonged the intestinal retention time of attached EcN via hitchhiking delivery. a) GPM were stained with DiI (red fluorescence membrane dye), and Caco-2 cells were stained with DiO (green fluorescence membrane dye). GPM (red fluorescence) were incubated with Caco-2 cells (green fluorescent) and LPS treated Caco-2 cells (green fluorescent), respectively. After incubation for 1 h, the mixtures were imaged by CLSM. b) Flow cytometry analysis on the mixtures. Upper left quadrant: GPM. Bottom right quadrant: Caco-2 cell. Upper right quadrant: conjugate of GPM and Caco-2 cells. c) IBD rats were intragastrically administered with free Cy5 and Cy5 loaded GPM (Cy5-GPM) at a dose of 1 mg/kg, and the colon tissues were collected for IVIS imaging after administration for different times (6 h, 12 h and 24 h). d) Quantitative analysis on the Cy5 fluorescence intensity of colon tissues. e) IBD rats were intragastrically administered with free EcN and GPM-EcN at 10^8 CFU/kg of EcN for 12 h and 24 h, and the fluorescence intensity of GFP transferred EcN in intestinal tissues was imaged by IVIS. f) Quantitative analysis on the EcN fluorescence intensity of colon tissues. g) Colocalization of DiI stained GPM (red fluorescence) and GFP transferred EcN (green fluorescence) in IBD rat administered intragastrically with GPM-EcN for 36 h. Data are represented as the mean ± SD (n = 3). Two-way ANOVA with multiple comparison test was used for statistical analysis of (d) and (f). *P ≤ 0.05, **P ≤ 0.01 and ***P ≤ 0.001. (For interpretation of the references to color in this figure legend, the reader is referred to the Web version of this article.)

increased from 58.7% to 78.3%. The result verified the chemical attachment of GPM on inflammatory cells, and provided the potential for GPM hitchhiking delivery of attached EcN to inflammatory intestinal endothelial cells.

Subsequently, SD rat was administered with TNBS solution via a rectal catheter to induce colitis, and the constructed IBD rats were intragastrically administered with free Cy5 and Cy5 loaded GPM (Cy5-GPM) at a dose of 1 mg/kg. After administration for 6 h, 12 h and 24 h,

the colon tissues were collected for *ex vivo* imaging by *in vivo* imaging system (IVIS). As shown in Fig. 4c, the stomach of Cy5 treated rat showed strong red fluorescence intensity after administration for 6 h, and the intestine fluorescence intensity was weak and disappeared in less than 12 h. In comparison to free Cy5, IBD rat treated with Cy5-GPM showed a high fluorescence intensity in the colon's distal part at beginning, and the intestine fluorescence was still even detected after administration for 24 h. Semi-quantitative analysis showed that intestinal fluorescence intensity in Cy5-GPM treated rat was 7.6-fold higher than that of free Cy5 treated rat (Fig. 4d). This should be attributed to the chemical attachment of GPM to colitis mucosa, contributing to the enhanced intestinal adhesion and retention of GPM. Furthermore, DiI stained GPM (red fluorescence) and GFP transformed EcN (green fluorescence) were carried out to track their *in vivo* biodistribution. IBD rat was intragastrically administered with free EcN, and exhibited a small green fluorescence area in colon tissues after administration for 12 h and 24 h (Fig. 4e), indicating a short intestinal retention time. In contrast, GPM-EcN treated rat exhibited quite large green fluorescent area of EcN after administered with the same dose of EcN (108 CFU/kg), and the fluorescence intensity was 5.2-fold as high as that of free EcN treated rat after administration for 24 h (Fig. 4f). The result indicated that GPM-hitchhiking delivery of attached EcN prolonged the retention time of EcN in colitis tissue. Further co-localization analysis in colon tissue showed that the green fluorescence signal of EcN overlapped well with the red fluorescent GPM (Fig. 4g), confirming GPM went hand-in-hand with the attached EcN in the form of GPM-EcN conjugate to accumulated in colitis tissue. Collectively, these findings demonstrated that GPM had preferential adhesion to inflammatory colon mucosal epithelium, and carried the attached EcN in the form of GPM-EcN to accumulate in colitis tissue, achieving a high intestinal retention time and abundance of oral probiotics via GPM-hitchhiking delivery.

3.5. Combination therapy of GPM-EcN on IBD rat

Based on the results of anti-inflammation effect of GPM and hitchhiking delivery of EcN to colitis tissue, the combination therapeutic effect of GPM-EcN was evaluated in IBD rat. In comparison to normal rat, TNBS treated rat exhibited an obviously decreased body weight, shortened colon length and histological damage, indicating the successful construction of IBD rat model. Then, IBD rats were randomly and blindly separated into three groups (n = 3), and administered intragastrically with GPM, EcN, and GPM-EcN at a dose of 10^8 CFU/kg of EcN and 70 mg/kg of GPM, once every two days with a total of three doses (Fig. 5a). The changes of body weight (Fig. 5b) and colon length (Fig. 5c–d) were partially recovered in GPM treated rats, which confirmed the good therapeutic efficacy of GPM through cytokine sequestration. Free EcN also slightly alleviated IBD symptom. As expected, GPM-EcN conducted a best amelioration effect, which should be attributed to the enhanced colon accumulation of EcN for regulating gut microbiota in combination with the anti-inflammation effect of GPM. The disease activity index (DAI) of IBD rat was also decreased after GPM-EcN treatment (Fig. 5e), indicating a low macroscopically visible damage. Together with the HE staining on colon section (Fig. 5f), GPM-EcN treated rat showed least lesion comparable to that of control group (Fig. 5g), with regular fingerlike crypt structure, intact epithelia, and low inflammatory cell infiltration. Masson staining was further carried out (Fig. 5h), and intestinal fibrosis was inhibited in GPM-EcN treated rat, indicating that GPM-EcN remarkably promoted the repair of colon tissues. Although not significant, GPM partially ameliorated TNBS-induced colitis and related symptoms in comparison to IBD model rat with severe goblet cell loss, obvious inflammatory cell infiltration, and high degree of intestinal fibrosis.

The IBD-associated MPO activity in rat colon was analyzed by immunohistochemical staining. As shown in Fig. 6a, the fluorescence of MPO was obviously downregulated, while free EcN also slightly reduced MPO expression (Fig. 6b), demonstrating that GPM could alleviate oxidative stress to relieve IBD. Macrophage infiltration and inflammatory cytokine release played important roles in the IBD process. [41] Then, macrophage ($F4/80^+$ cells) in colon section was labeled, and a large number of fluorescent dots was observed in IBD rat (Fig. 6a). In contrast, GPM treatment obviously decreased the macrophage infiltration in colitis tissue (Fig. 6c). Furthermore, the high levels of proinflammatory cytokines (TNF-α, IL-1β and IL-6) in colitis tissue was efficiently downregulated by GPM (Fig. 6d) and the low level of anti-inflammatory factor (IL-10) was upregulated, which further demonstrating the excellent anti-inflammation effect of GPM. In comparison, free EcN moderately inhibited macrophage infiltration and cytokine expression. Subsequently, the effect of GPM and EcN on colonic epithelial cell and barrier was investigated. ZO-1 and occludin were the main tight junction associated proteins, and mainly maintained the function of intestinal epithelium and the integrity of intestinal barrier. [42,43] According to the results of immunohistochemical staining, GPM upregulated the expression of ZO-1 and occludin (Fig. 6e) in colitis tissue of IBD rat, and free EcN also slightly improved their expression (Fig. 6f and g). In addition, IBD rat showed an increased vimentin in colon tissue, which suppressed the production of ROS and autophagy and contributed to IBD development (Fig. S6). GPM obviously reduced vimentin level in colitis tissue. The results indicated the key role of GPM in the restoration of colonic epithelium due to its anti-inflammation effect. As expect, the combination therapy of GPM and EcN contributed to the excellent anti-oxidation ability, anti-inflammation effect, intestinal barrier repair of GPM-EcN conjugate. Taken together, GPM-EcN effectively relieved acute IBD in rat, and GPM in the form of single treatment also exhibited moderately alleviation in IBD symptom. Of note, free EcN only slightly improve IBD symptom with a delayed therapeutic response time. Thus, EcN was supposed to maximize the therapeutic efficacy of GPM on IBD rats and the mechanism was studied by intestinal flora and metabolite analysis.

3.6. Regulatory effect of GPM-EcN on gut microbiome

Due to the improved intestine abundance of EcN, the effect of GPM-EcN conjugation on gut microbiota regulation was further investigated by 16S ribosomal RNA (rRNA) gene sequencing of the V4–V5 regions. Alpha diversity analysis showed that TNBS-induced colitis rat had the lowest bacterial richness in comparison to that of normal rat, reflected in the observed operational taxonomic units (OTUs) (Fig. 7a). In all treated rats, the bacteria richness was increased, and EcN and GPM-EcN containing probiotics exhibited closer richness to normal rat in comparison to that of free GPM. Further analysis with nonmetric multidimensional scaling (NMDS) plots revealed that the bacterial community was significantly changed in IBD rat, and EcN and GPM-EcN shifted the bacterial community composition and structure close to those of normal rat (Fig. 7b). In contrast, the bacterial community was only slightly normalized after GPM treatment. The histogram showed that the most abundant bacteria in normal rats, IBD rats and all treated rats were Firmicutes, Bacteroidota, Proteobacteria, Verrucomicrobiota, Actinobacteria, and Dsulfobacterota (Fig. S7). Furthermore, the relative abundance of dominant phyla was reflected by heatmap (Fig. 7c), and three phyla (Firmicutes, Bacteroidota and Protrobacteria) displayed significant difference among groups. TNBS treatment significantly upregulated the ratio of Firmicutes to Bacteroidota (Firmicutes/Bacteroidota), which contribute to colitis pathogenesis and intestinal barrier damage (Fig. 7d). [44,45] Treatment with GPM-EcN clearly recovered the upregulated ratio of Firmicutes/Bacteroidota to normal level, and exhibited a better performance than that of both GPM and free EcN. In addition, previous study showed Proteobacteria was a major source of translocated antigen LPS, [46] and GPM-EcN and free EcN both increased the relative abundance of Proteobacteria in comparison to that of IBD rat, while GPM had little effect on the abundance of Proteobacteria (Fig. 7d).

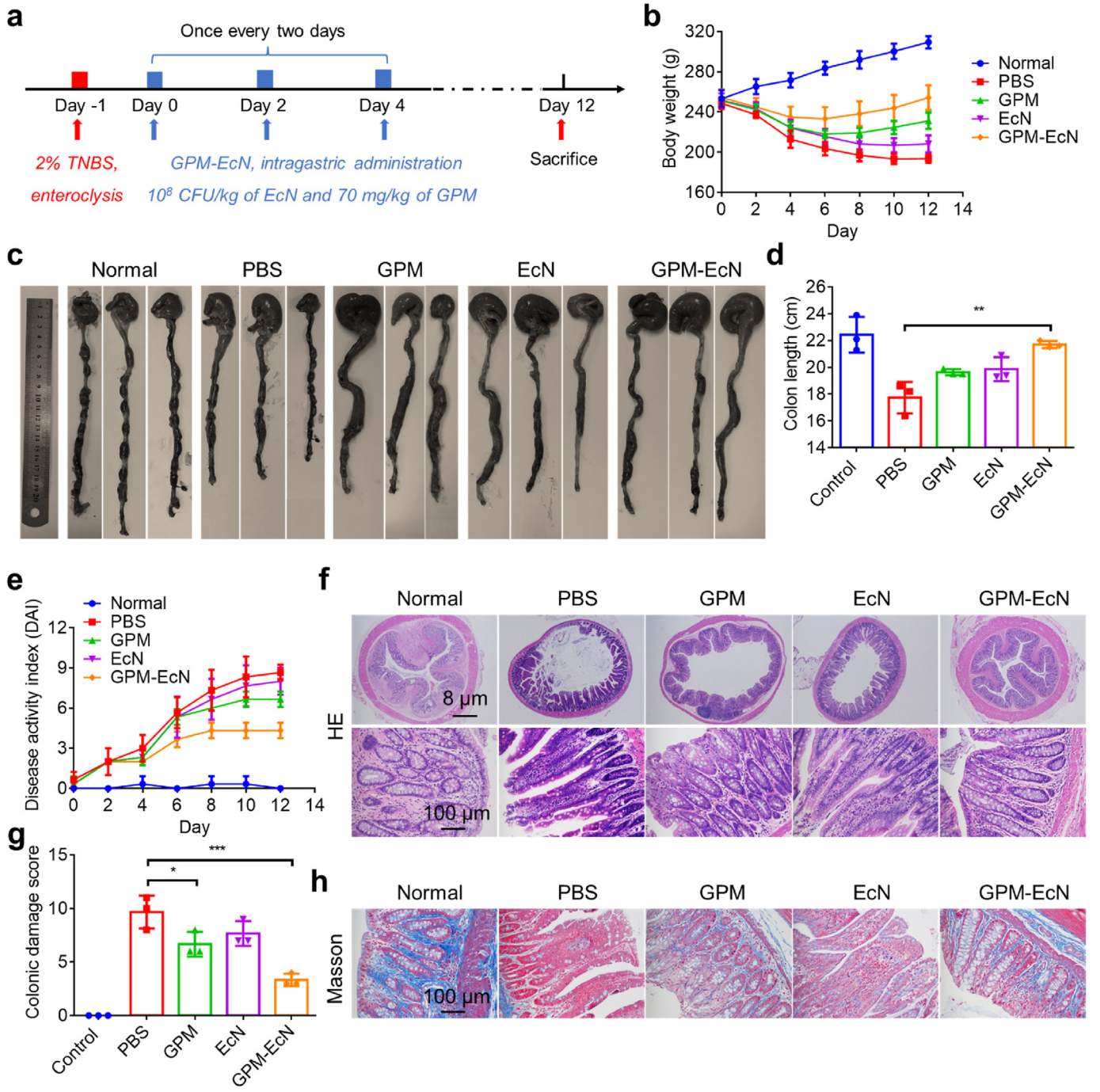

Fig. 5. GPM-EcN recovered colitis symptom of IBD rat via efficient cytokine neutralization effect of GPM and gut microbiota modulation of EcN. a) Schematic illustration of therapeutic protocol. IBD rats were randomly and blindly separated into three groups (n = 3), and intragastrically administered with GPM, EcN, and GPM-EcN at 10^8 CFU/kg of EcN and 70 mg/kg of GPM, once every two days with a total of three doses. b) The change of body weight was recorded. c) All rats were sacrificed at Day 12 and the colon tissues were collected for photo imaging. d) The colon length was recorded. e) The changes of rat DAI during treatment. f) HE staining was conducted in colon sections from all treated rats at magnification of 2x10 and 2x100, and representative image was shown. G) Quantification on the colonic damage score. h) Masson staining was conducted in colon section and representative image was shown. Data are represented as the mean ± SD (n = 3). One-way ANOVA with multiple comparison test was used for statistical analyses of (d) and (g). *P ≤ 0.05, **P ≤ 0.01 and ***P ≤ 0.001.

This result indicated that oral administration of probiotics (EcN), played a key role in recovering gut bacterial community. GPM also slightly improved intestinal flora homeostasis due to its anti-inflammation effect, and combined with EcN to contribute to a better microbiota regulation in the form of GPM-EcN conjugate.

Finally, a total of 16,753 peaks representing 941 and 858 metabolites in positive and negative ion modes were identified by metabolomics analysis. The heatmap conducted from each rat showed that normal rat had highly relationship with rat treated with EcN and GPM-EcN, respectively (Fig. S8). Besides, PCA analysis was conducted to determine the similarity in metabolites among groups (Fig. 7e). The results showed that the cluster of IBD rat was far away from the normal rat. Similarly, GPM also normalized bacterial metabolites, but the modulation effect was relative weak, which should be directly attributed to the

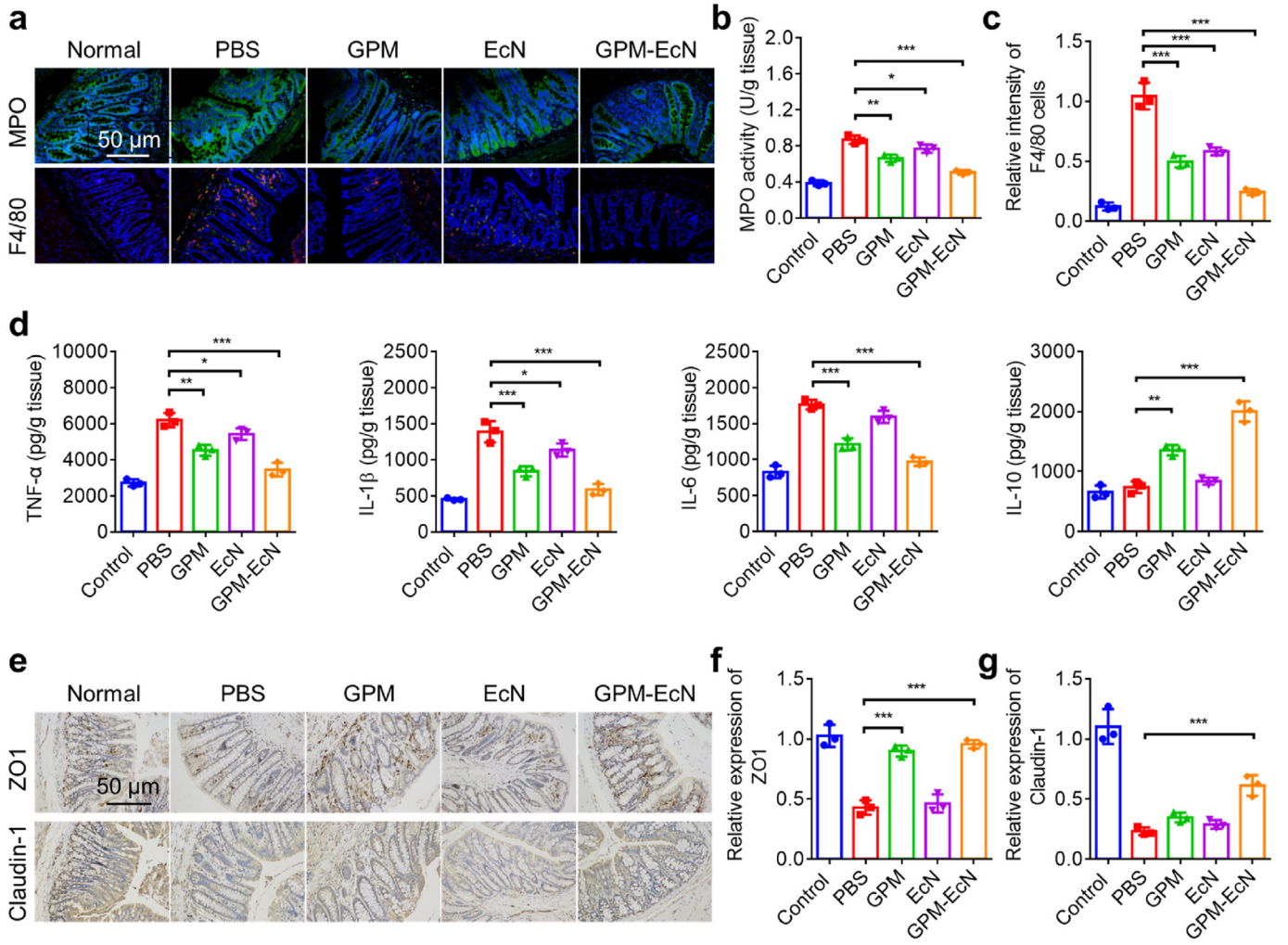

Fig. 6. GPM-EcN ameliorated colon inflammation and repaired intestinal barrier. a) Fluorescence imaging on MPO labeled colon section and F4/80 labeled colon section from all treated rats. b) MPO activity in colon tissue was determined by Elisa kit. c) The infiltration ratio of macrophage (F4/80^{+} cells) in colon tissue was semi-quantified from fluorescence image. d) The levels of inflammatory cytokines (TNF-α, IL-1β, IL-6 and IL10) in colon tissue from treated rats were measured by Elisa kits. e) Immunohistochemical analysis on the expression of ZO-1 and Claudin-1 in colon tissues collected from treated rats. f) Quantitative analysis of relative expression of ZO1. g) Quantitative analysis of relative expression of Claudin-1. Data are represented as the mean ± SD (n = 3). One-way ANOVA with multiple comparison test was used for statistical analysis of (b), (c), (d) (f) and (g). *P ≤ 0.05, **P ≤ 0.01 and ***P ≤ 0.001.

slight microbiota regulation. Furthermore, differential acid metabolites were selected with $P < 0.05$, and shown in Table S1. TNBS treatment upregulated the intestinal production of arachidonic acid, citric acid, corchorifatty acid D, formiminoglutamic acid, galactonic acid, ganoderic acid F, hexadecanedioic acid, and hippuric acid, which resulted in the proinflammatory response, pain, and fever, [47] and downregulated the production of docosapentaenoic acid, dodecanedioic acid, ganoderic acid H, ganoderic acid K, and gentisic acid, which could reduce intestinal inflammatory disorder. [48] After treatment with GPM, EcN and GPM-EcN, the cluster moved close to the normal group, and rat treated with GPM-EcN and free EcN even had a more similar dot distribution with normal rat in comparison to that of GPM, indicating GPM-EcN and free EcN recovered acid metabolites to normal level. Therefore, the therapeutic effects of GPM-EcN on colitis should be partially attributed to the gut microbiota regulation, in which free EcN played a key role assisted by GPM. Free EcN improved bacterial diversity, and shifted the microbiota community and acid metabolites to an anti-inflammatory phenotype, which combined with the anti-inflammation effect of GPM to contribute to an efficient anti-IBD treatment of GPM-EcN. Collectively, these results indicated that the GPM-EcN conjugate restored the intestinal homeostasis of gut microbiota and acid metabolites in IBD rat, in addition to regulating oxidative stress, inflammation level and intestinal barrier repair.

3.7. *In vivo* biosafety of GPM-EcN treatment

Encouraged by the efficient therapeutic efficacy of GPM-EcN conjugate, the *in vivo* safety was evaluated in normal rat orally treated with GPM-EcN at a dose of 10^8 CFU/kg of EcN and 70 mg/kg of GPM, once every two days with a total of three doses. After further treatment for one week, HE staining on the collected organs (heart, liver, spleen, lung and kidney) showed no histological damage in GPM-EcN treated rat, comparable to that of normal rat (Fig. S9a). A complete blood count was conducted, and the number of white blood cells (WBC), red blood cells (RBC) and platelets was also similar between GPM-EcN treated rat and normal rat (Fig. S9b). In addition, serum biochemistry analysis exhibited that the serum levels of ALT, AST, BUN and UA in GPM-EcN treated rat almost did not change in comparison to that of normal rat (Fig. S9c and S9d), indicating GPM-EcN treated had no effect on the liver function and kidney function. Thus, these results demonstrated that oral GPM-EcN

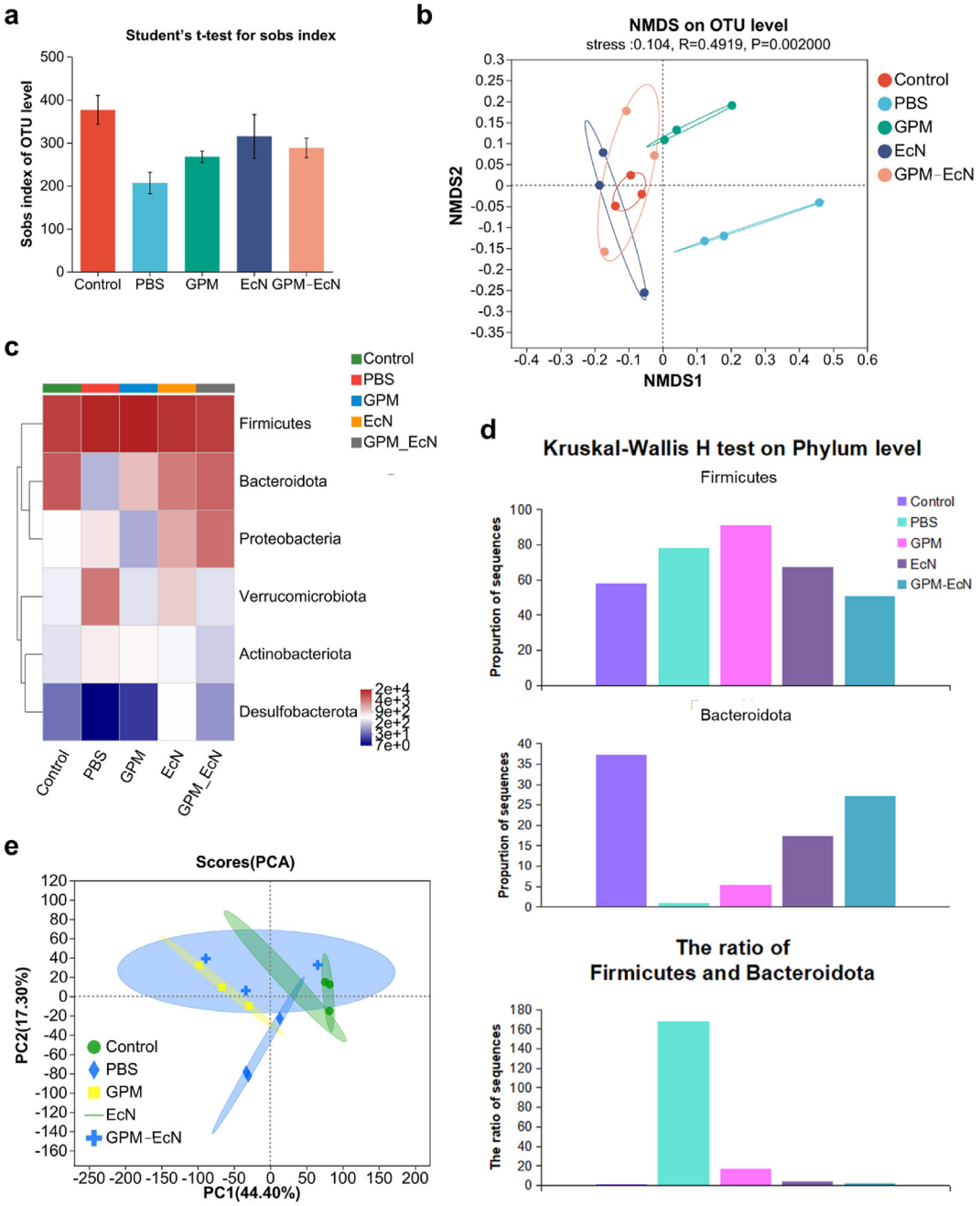

Fig. 7. GPM-EcN altered the intestinal microbial community composition and structure. a) Estimation of microbial community diversity based on sobs index. b) NMDS analysis presenting the β diversity of intestinal microbes. c) The heatmap showing the relative abundance of dominant phyla for each sample. d) Krusal-Wallis H test showing the significant changed phyla. e) PCA analysis illustrating the differences of microbial metabolites.

treatment did not induced any *in vivo* toxicity or side effect, which should be attributed to the biocompatible raw materials derived from self-cell and probiotics.

4. Conclusion

In light of the current limitations of immune cell membrane coated nanomedicine used for anti-inflammation in IBD treatment, a natural GPM with intact macrophage morphology and membrane structure was developed via intracellular gelation technology. The receptor content in the membrane GPM, especially for those binding with multiple cytokines, was similar to that of source macrophages, and GPM efficiently absorbed and neutralized different types of cytokines (TNF-α and IL-1β) without activation into M1 type. In the classic model of inflammatory colon cells, co-treatment with GPM efficiently inhibited cell death, ROS generation and apoptotic rate, and then reduced cytokine release in LPS treated Caco2 cells. As is well known, TLR4 is an indispensable receptor for LPS, which plays an important role in the immune response to bacterial infection. [49] LPS-TLR4 receptor complexation on macrophages activates NF-κB signaling pathway, and leads to the release of inflammatory factors, which eventually initiated the activation of immune cell and inflammatory response. [50] Due to the specific recognition of TLR4 and LPS in the surface of GPM and EcN, GPM-EcN conjugate was easily constructed. Due to GPM-hitchhiking delivery to colitis tissue, GPM-EcN increased the accumulation rate of attached EcN in the intestine after oral administration, which was ~4.8-fold higher than that of free EcN.

Colocalization analysis on intestine section further confirmed the hand-in-hand delivery of transporting GPM and anchored EcN. Subsequently, IBD rat treated with GPM reduced intestine inflammation level, and GPM-EcN significantly ameliorated intestine damage. In addition, accumulated EcN regulated the intestinal microbial communities and increased the ratio of Firmicutes to Bacteroidota and the abundance of Proteobacteria, which were important microbes to maintain intestinal homeostasis. Further analysis of intestine metabolite revealed the normalization of gut microbiota by GPM-EcN treatment downregulated the production of proinflammatory acid metabolites, and upregulated the production of acid metabolites which recovered the intestinal inflammatory disorder. The cytokine neutralization effect of GPM and gut microbiota modulation of EcN contributed to an efficient anti-IBD treatment of GPM-EcN conjugate.

It was reported that liquid nitrogen freezing treatment was utilized to prepare dead cell for diverse biomedical applications. [51] However, the cell after liquid nitrogen freezing treatment was very unstable, and easy to be broken down into cellular fragments. In comparison, intracellular hydrogel in our study served as an ideal cytoskeleton to support the stability of cell structure, which maintained the intact cellular morphology and membrane protein of GPM. Overall, this study achieved three highlights in the oral treatment of IBD. Firstly, nanomaterials with enzymatic catalytic activities had been used to neutralize reactive oxygen species (ROS), suppress inflammation, or scavenge proinflammatory cell-free DNA (cfDNA) for IBD treatment, which however were artificially constructed via complicated process and limited by potential immunogenicity when applicated *in vivo*. [52,53] In comparison to the catalytic nanomaterials, this study developed intracellular hydrogelation technology, and constructed GPM without membrane isolation and re-assembly process to maintain the intact membrane structure for efficient neutralization towards multiple intestine cytokines. Secondly, it provided a facile and quick construction methodology to prepare GPM-EcN conjugate via specific recognition effect, and this GPM-hitchhiking delivery system addressed the clinical issue of quick probiotics clearance through oral administration. GPM adhered on the colitis mucosa in response to inflammation signal, and contributed to the hitchhiking delivery of attached EcN to colitis tissue and prolonging the retention time. Finally, bacterial metabolite regulation by EcN combined with the anti-inflammatory effect of GPM significantly alleviated IBD symptom. Increased intestine ratio of Firmicutes to Bacteroidota and abundance of Proteobacteria caused by EcN regulation improve production of anti-inflammatory acid metabolites, which maximized the amelioration effect of GPM on IBD symptom. This study transferred the hydrogel synthesis to intracellular cytoplasm, and came to a new insight of conjugating strategy of GPM and probiotics for clinical IBD treatment.

In addition to peritoneal macrophage, inflammatory bowel tissue always involved high infiltration of other immune cells, such as neutrophil and T cell, [54,55] and this intracellular gelation platform could also be applicated in these cells for anti-inflammation therapy. Moreover, besides singlet EcN, multiple probiotics could also be attached in the surface of GPM, and contributed to multiple regulation on intestinal microbiota. This study described a modular GPM-EcN conjugate for combinational IBD treatment that showed much improved therapeutic efficacy in comparison to traditional monoclonal antibody and free EcN, including multiple cytokines neutralization, surface binding capacity for probiotics loading, interaction with inflammatory bowel tissue for longtime retention, combination therapy of anti-inflammation and gut microbiota modulation, derived from self-cell without evidence of toxicity, and simplified production for easy accessibility.

CRediT authorship contribution statement

Jingzhe Wang: Methodology, Data curation, Writing- Original draft preparation. Dini Hu: Methodology, Data curation. Qian Chen: Methodology, Data curation. Tonggong Liu and Xiaoting Zhou: Methodology, Resources. Yong Xu: Conceptualization, Resources. Cheng Gao, Dayong Gu and Hongzhong Zhou Conceptualization, Supervision, Resources, Writing - Review & Editing.

Declaration of competing interest

The authors declare that they have no known competing financial interests or personal relationships that could have appeared to influence the work reported in this paper.

Data availability

No data was used for the research described in the article.

Acknowledgement

The authors acknowledged the financial support from the National Key Research and Development Program of China (No.2022YFC2302700), the National Natural Science Foundation of China (No. 32001016, No. 82203870), the GuangDong Basic and Applied Basic Research Foundation (No. 2020A1515110871, No. 2020B1111160001, No.2021A1515220084, No. 2022A1515220006), the China Postdoctoral Science Foundation (No. 2022M722204), the Shenzhen Science and Technology Foundation (No. RCBS20200714114856016, No. JCYJ20210324103204011, No. GJHZ20200731095604013, No. ZDSYS20210623092001003).

Appendix A. Supplementary data

Supplementary data to this article can be found online at https://doi.org/10.1016/j.mtbio.2023.100679.

References

[1] J.L. Alexander, G.W. Moran, D.R. Gaya, T. Raine, A. Hart, N.A. Kennedy, J.O. Lindsay, J. MacDonald, J.P. Segal, S. Sebastian, SARS-CoV-2 vaccination for patients with inflammatory bowel disease: a British Society of Gastroenterology Inflammatory Bowel Disease section and IBD Clinical Research Group position statement, Lancet Gastroenterol. Hepatol. 6 (3) (2021) 218–224.
[2] R. Banerjee, P. Pal, J.W.Y. Mak, S.C. Ng, Challenges in the diagnosis and management of inflammatory bowel disease in resource-limited settings in Asia, Lancet Gastroenterol. Hepatol. 5 (12) (2020) 1076–1088.
[3] J.K. Gustafsson, M.E. Johansson, The role of goblet cells and mucus in intestinal homeostasis, Nat. Rev. Gastroenterol. Hepatol. (2022) 1–19.
[4] P. Paone, P.D. Cani, Mucus barrier, mucins and gut microbiota: the expected slimy partners? Gut 69 (12) (2020) 2232–2243.
[5] M. Mahapatro, L. Erkert, C. Becker, Cytokine-mediated crosstalk between immune cells and epithelial cells in the gut, Cells 10 (1) (2021) 111.
[6] J.V. Patankar, C. Becker, Cell death in the gut epithelium and implications for chronic inflammation, Nat. Rev. Gastroenterol. Hepatol. 17 (9) (2020) 543–556.
[7] I. Schoultz, Å.V. Keita, The intestinal barrier and current techniques for the assessment of gut permeability, Cells 9 (8) (2020) 1909.
[8] Y. Pu, X. Fan, Z. Zhang, Z. Guo, Q. Pan, W. Gao, K. Luo, B. He, Harnessing polymer-derived drug delivery systems for combating inflammatory bowel disease, J. Contr. Release 354 (2023) 1–18.
[9] S. Vermeire, P.L. Lakatos, T. Ritter, S. Hanauer, B. Bressler, R. Khanna, K. Isaacs, S. Shah, A. Kadva, H. Tyrrell, Etrolizumab for maintenance therapy in patients with moderately to severely active ulcerative colitis (LAUREL): a randomised, placebo-controlled, double-blind, phase 3 study, Lancet Gastroenterol. Hepatol. 7 (1) (2022) 28–37.
[10] B. Barberio, D.J. Gracie, C.J. Black, A.C. Ford, Efficacy of biological therapies and small molecules in induction and maintenance of remission in luminal Crohn's disease: systematic review and network meta-analysis, Gut (2022).
[11] H. Yanai, A. Levine, A. Hirsch, R.S. Boneh, U. Kopylov, H.B. Eran, N.A. Cohen, Y. Ron, I. Goren, H. Leibovitzh, The Crohn's disease exclusion diet for induction and maintenance of remission in adults with mild-to-moderate Crohn's disease (CDED-AD): an open-label, pilot, randomised trial, Lancet Gastroenterol. Hepatol. 7 (1) (2022) 49–59.
[12] G. Maiti, J. Frikeche, C.Y.-M. Lam, A. Biswas, V. Shinde, M. Samanovic, J.C. Kagan, M.J. Mulligan, S. Chakravarti, Matrix lumican endocytosed by immune cells controls receptor ligand trafficking to promote TLR4 and restrict TLR9 in sepsis, Proc. Natl. Acad. Sci. USA 118 (27) (2021), e2100999118.
[13] J. Zhou, A.V. Kroll, M. Holay, R.H. Fang, L. Zhang, Biomimetic nanotechnology toward personalized vaccines, Adv. Mater. 32 (13) (2020), 1901255.
[14] W.-L. Liu, M.-Z. Zou, S.-Y. Qin, Y.-J. Cheng, Y.-H. Ma, Y.-X. Sun, X.-Z. Zhang, Recent advances of cell membrane-coated nanomaterials for biomedical applications, Adv. Funct. Mater. 30 (39) (2020), 2003559.

[15] P. Dash, A.M. Piras, M. Dash, Cell membrane coated nanocarriers - an efficient biomimetic platform for targeted therapy, J. Contr. Release 327 (2020) 546–570.
[16] M. Wang, Y. Xin, H. Cao, W. Li, Y. Hua, T.J. Webster, C. Zhang, W. Tang, Z. Liu, Recent advances in mesenchymal stem cell membrane-coated nanoparticles for enhanced drug delivery, Biomater. Sci. 9 (4) (2021) 1088–1103.
[17] P. Dash, A.M. Piras, M. Dash, Cell membrane coated nanocarriers-an efficient biomimetic platform for targeted therapy, J. Contr. Release 327 (2020) 546–570.
[18] D. Nie, Z. Dai, J. Li, Y. Yang, Z. Xi, J. Wang, W. Zhang, K. Qian, S. Guo, C. Zhu, Cancer-cell-membrane-coated nanoparticles with a yolk–shell structure augment cancer chemotherapy, Nano Lett. 20 (2) (2019) 936–946.
[19] Y. Jiang, N. Krishnan, J. Zhou, S. Chekuri, X. Wei, A.V. Kroll, C.L. Yu, Y. Duan, W. Gao, R.H. Fang, Engineered cell-membrane-coated nanoparticles directly present tumor antigens to promote anticancer immunity, Adv. Mater. 32 (30) (2020), 2001808.
[20] D.A. Schupack, R.A. Mars, D.H. Voelker, J.P. Abeykoon, P.C. Kashyap, The promise of the gut microbiome as part of individualized treatment strategies, Nat. Rev. Gastroenterol. Hepatol. 19 (1) (2022) 7–25.
[21] A. Lavelle, H. Sokol, Gut microbiota-derived metabolites as key actors in inflammatory bowel disease, Nat. Rev. Gastroenterol. Hepatol. 17 (4) (2020) 223–237.
[22] P. Spanogiannopoulos, T.S. Kyaw, B.G. Guthrie, P.H. Bradley, J.V. Lee, J. Melamed, Y.N.A. Malig, K.N. Lam, D. Gempis, M. Sandy, Host and gut bacteria share metabolic pathways for anti-cancer drug metabolism, Nat. Microbiol. 7 (10) (2022) 1605–1620.
[23] J. Yang, G. Zhang, M. Peng, S. Tan, S. Ge, X. Yang, Y. Liang, Z. Wen, L. Xie, T. Zhou, Bionic regulators break the ecological niche of pathogenic bacteria for modulating dysregulated microbiome in colitis, Adv. Mater. 34 (39) (2022), 2204650.
[24] R. Zhu, T. Lang, W. Yan, X. Zhu, X. Huang, Q. Yin, Y. Li, Gut microbiota: influence on carcinogenesis and modulation strategies by drug delivery systems to improve cancer therapy, Adv. Sci. 8 (10) (2021), 2003542.
[25] J. Xu, J. Xu, T. Shi, Y. Zhang, F. Chen, C. Yang, X. Guo, G. Liu, D. Shao, K.W. Leong, Probiotic-inspired nanomedicine restores intestinal homeostasis in colitis by regulating redox balance, immune responses, and the gut microbiome, Adv. Mater. (2022), 2207890.
[26] Y. Qin, R. Zhao, H. Qin, L. Chen, H. Chen, Y. Zhao, G. Nie, Colonic mucus-accumulating tungsten oxide nanoparticles improve the colitis therapy by targeting Enterobacteriaceae, Nano Today 39 (2021), 101234.
[27] M.T. Buss, P. Ramesh, M.A. English, A. Lee-Gosselin, M.G. Shapiro, Spatial control of probiotic bacteria in the gastrointestinal tract assisted by magnetic particles, Adv. Mater. 33 (17) (2021), 2007473.
[28] S. Lin, S. Mukherjee, J. Li, W. Hou, C. Pan, J. Liu, Mucosal immunity–mediated modulation of the gut microbiome by oral delivery of probiotics into Peyer's patches, Sci. Adv. 7 (20) (2021), eabf0677.
[29] F. Wu, J. Liu, Decorated bacteria and the application in drug delivery, Adv. Drug Deliv. Rev. (2022), 114443.
[30] B.O. Fabriek, R. van Bruggen, D.M. Deng, A.J. Ligtenberg, K. Nazmi, K. Schornagel, R.P. Vloet, C.D. Dijkstra, T.K. van den Berg, The macrophage scavenger receptor CD163 functions as an innate immune sensor for bacteria, Blood, J. Am. Soci. Hematol. 113 (4) (2009) 887–892.
[31] S.B. Han, Y.D. Yoon, H.J. Ahn, H.S. Lee, C.W. Lee, W.K. Yoon, S.K. Park, H.M. Kim, Toll-like receptor-mediated activation of B cells and macrophages by polysaccharide isolated from cell culture of Acanthopanax senticosus, Int. Immunopharm. 3 (9) (2003) 1301–1312.
[32] I.E. Antonescu, K.F. Rasmussen, S. Neuhoff, X. Fretté, M. Karlgren, C.A. Bergström, C.U. Nielsen, B. Steffansen, The permeation of Acamprosate is predominantly caused by Paracellular diffusion across Caco-2 cell monolayers: a Paracellular modeling approach, Mol. Pharm. 16 (11) (2019) 4636–4650.
[33] N. Powell, E. Pantazi, P. Pavlidis, A. Tsakmaki, K. Li, F. Yang, A. Parker, C. Pin, D. Cozzetto, D. Minns, Interleukin-22 orchestrates a pathological endoplasmic reticulum stress response transcriptional programme in colonic epithelial cells, Gut 69 (3) (2020) 578–590.
[34] C. Echalier, L. Valot, J. Martinez, A. Mehdi, G. Subra, Chemical cross-linking methods for cell encapsulation in hydrogels, Mater. Today Commun. 20 (2019), 100536.
[35] K. Gwon, I. Han, S. Lee, Y. Kim, D.N. Lee, Novel metal–organic framework-based photocrosslinked hydrogel system for efficient antibacterial applications, ACS Appl. Mater. Interfaces 12 (18) (2020) 20234–20242.
[36] Z. Xie, Y. Wang, J. Huang, N. Qian, G. Shen, L. Chen, Anti-inflammatory activity of polysaccharides from Phellinus linteus by regulating the NF-κB translocation in LPS-stimulated RAW264. 7 macrophages, Int. J. Biol. Macromol. 129 (2019) 61–67.
[37] J. Tulkens, G. Vergauwen, J. Van Deun, E. Geeurickx, B. Dhondt, L. Lippens, M.-A. De Scheerder, I. Miinalainen, P. Rappu, B.G. De Geest, Increased levels of systemic LPS-positive bacterial extracellular vesicles in patients with intestinal barrier dysfunction, Gut 69 (1) (2020) 191–193.
[38] X.-X. Wu, X.-L. Huang, R.-R. Chen, T. Li, H.-J. Ye, W. Xie, Z.-M. Huang, G.-Z. Cao, Paeoniflorin prevents intestinal barrier disruption and inhibits lipopolysaccharide (LPS)-induced inflammation in Caco-2 cell monolayers, Inflammation 42 (6) (2019) 2215–2225.
[39] L. Dong, J. Xie, Y. Wang, H. Jiang, K. Chen, D. Li, J. Wang, Y. Liu, J. He, J. Zhou, Mannose ameliorates experimental colitis by protecting intestinal barrier integrity, Nat. Commun. 13 (1) (2022) 1–17.
[40] C.J. Greene, J.A. Nguyen, S.M. Cheung, C.R. Arnold, D.R. Balce, Y.T. Wang, A. Soderholm, N. McKenna, D. Aggarwal, R.I. Campden, Macrophages disseminate pathogen associated molecular patterns through the direct extracellular release of the soluble content of their phagolysosomes, Nat. Commun. 13 (1) (2022) 1–17.
[41] B. Ruder, C. Becker, At the forefront of the mucosal barrier: the role of macrophages in the intestine, Cells 9 (10) (2020) 2162.
[42] M. Hussain, M.U. Ijaz, M.I. Ahmad, I.A. Khan, S.A. Brohi, A.U. Shah, K.I. Shinwari, D. Zhao, X. Xu, G. Zhou, Meat proteins in a high-fat diet have a substantial impact on intestinal barriers through mucus layer and tight junction protein suppression in C57BL/6J mice, Food Funct. 10 (10) (2019) 6903–6914.
[43] T. Suzuki, Regulation of the intestinal barrier by nutrients: the role of tight junctions, Anim. Sci. J. 91 (1) (2020), e13357.
[44] R. Cao, X. Wu, H. Guo, X. Pan, R. Huang, G. Wang, J. Liu, Naringin exhibited therapeutic effects against DSS-induced mice ulcerative colitis in intestinal barrier–dependent manner, Molecules 26 (21) (2021) 6604.
[45] N. Chaput, P. Lepage, C. Coutzac, E. Soularue, K. Le Roux, C. Monot, L. Boselli, E. Routier, L. Cassard, M. Collins, Baseline gut microbiota predicts clinical response and colitis in metastatic melanoma patients treated with ipilimumab, Ann. Oncol. 28 (6) (2017) 1368–1379.
[46] T. Alhmoud, A. Kumar, C.-C. Lo, R. Al-Sadi, S. Clegg, I. Alomari, T. Zmeili, C.D. Gleasne, K. Mcmurry, A.E.K. Dichosa, Investigating intestinal permeability and gut microbiota roles in acute coronary syndrome patients, Human Microbiome J. 13 (2019), 100059.
[47] F. Yin, X. Huang, X. Lin, T.F. Chan, K.P. Lai, R. Li, Analyzing the synergistic adverse effects of BPA and its substitute, BHPF, on ulcerative colitis through comparative metabolomics, Chemosphere 287 (2022), 132160.
[48] Q. Liu, B. Li, Y. Li, Y. Wei, B. Huang, J. Liang, Z. You, Y. Li, Q. Qian, R. Wang, Altered faecal microbiome and metabolome in IgG4-related sclerosing cholangitis and primary sclerosing cholangitis, Gut 71 (5) (2022) 899–909.
[49] A.H. Lee, C. Ledderose, L. Xiaoou, C.J. Slubowski, K. Sueyoshi, L. Staudenmaier, Y. Bao, J. Zhang, W.G. Junger, ATP release is required for Toll-like receptor-induced monocyte/macrophage activation, NLRP3 inflammasome signaling, IL-1β production, and the host immune response to infection, Crit. Care Med. 46 (12) (2018) e1183.
[50] L.A. O'Neill, A.G. Bowie, The family of five: TIR-domain-containing adaptors in Toll-like receptor signalling, Nat. Rev. Immunol. 7 (5) (2007) 353–364.
[51] T. Ci, H. Li, G. Chen, Z. Wang, J. Wang, P. Abdou, Y. Tu, G. Dotti, Z. Gu, Cryo-shocked cancer cells for targeted drug delivery and vaccination, Sci. Adv. 6 (50) (2020), eabc3013.
[52] M. Li, J. Liu, L. Shi, C. Zhou, M. Zou, D. Fu, Y. Yuan, C. Yao, L. Zhang, S. Qin, Gold nanoparticles-embedded ceria with enhanced antioxidant activities for treating inflammatory bowel disease, Bioact. Mater. 25 (2023) 95–106.
[53] J. Liu, Y. Wang, W.J. Heelan, Y. Chen, Z. Li, Q. Hu, Mucoadhesive probiotic backpacks with ROS nanoscavengers enhance the bacteriotherapy for inflammatory bowel diseases, Sci. Adv. 8 (45) (2022), eabp8798.
[54] S. Ronchetti, M. Gentili, E. Ricci, G. Migliorati, C. Riccardi, Glucocorticoid-induced Leucine zipper as a Druggable target in inflammatory bowel diseases, Inflamm. Bowel Dis. 26 (7) (2020) 1017–1025.
[55] I. Tindemans, M.E. Joosse, J.N. Samsom, Dissecting the heterogeneity in T-cell mediated inflammation in IBD, Cells 9 (1) (2020) 110.